

Biophysical and Transfection Studies of the diC₁₄-Amidine/DNA Complex

Vadim Cherezov,* Hong Qiu,* Veronique Pector,[†] Michel Vandenbranden,[†] Jean-Marie Ruyschaert,[†] and Martin Caffrey*

*Biochemistry, Biophysics, and Chemistry, The Ohio State University, 100 West 18th Avenue, Columbus, Ohio 43210 USA; and [†]Structure et Fonction des Membranes Biologiques, Université Libre de Bruxelles, Campus Plaine CP 206/2, B-1050 Brussels, Belgium

ABSTRACT Liposomes of the synthetic cationic lipid, *N*-*t*-butyl-*N'*-tetradecylamino-propionamidine (diC₁₄-amidine), efficiently ports DNA into mammalian cells in the absence of other (neutral) lipids. The compositional simplicity of this transfection mix makes it attractive from a formulation perspective. We have used low- and wide-angle x-ray diffraction and polarized light microscopy to characterize the thermotropic phase behavior and microstructure of diC₁₄-amidine and of the lipid/DNA (circular plasmid, 5.4 kb) complex with a view to understanding the structure of the complex and its role in transfection. Upon heating, the lipid in buffer undergoes a lamellar crystalline (L_c , $d_{001} = 41.7 \text{ \AA}$)-to-lamellar liquid crystal (L_α^c , d_{001} depends on hydration and T) transition at $\sim 40^\circ\text{C}$. Sonicated lipid vesicles with a reported transition temperature of $\sim 23^\circ\text{C}$ complex with DNA. Complex formation is complete at a DNA/lipid mole ratio (ρ) of 0.8. Adding DNA to the lipid causes d_{001} of the multilayered complex to drop from 52 to 49 \AA as ρ rises from 0.03 to 1.64. The minimal DNA-DNA duplex separation observed is 26 \AA , consistent with the close packing of B-DNA. Lipid bilayers in the complex undergo a lamellar gel (L_β^c)-to- L_α^c (superscript c refers to complex) transition at $\sim 23^\circ\text{C}$. Transfection efficiency was maximized at $\rho = 0.4$. The structure and transfection data combined suggest that densely packaged DNA in a net positively charged complex is essential for transfection.

INTRODUCTION

Transfection is a process whereby nucleic acid, primarily as recombinant DNA of known sequence and functionality, is placed in a target cell. Transfection is implemented typically to modify the gene complement of the recipient cell for use in controlled expression. The means by which “foreign” DNA can be packaged and delivered to a host cell are many and varied. The most efficient of these makes use of viruses. But viral vectors have their shortcomings not the least of which is the potential for disease transmission.

Cationic lipids are naturally attracted to and spontaneously form complexes with polyanionic DNA. Such complexes, referred to variously as lipoplexes, have proven useful as transfection vehicles both in vitro (El Ouahabi et al., 1996; Felgner et al., 1994; Gao and Huang, 1995; Liu et al., 1997; Ruyschaert et al., 1994) and in vivo (Zelphati et al., 1998; Hoffman and Figlin, 2000). Lipoplexes offer several advantages in that they provide a high DNA packing density, they are less immunogenic, and are likely to be able to port DNA of considerably larger size than their viral counterparts (Lasic, 1997; Felgner, 1997; Logan et al., 1995; Blezinger et al., 1999). The possibility of targeting lipidic carriers to specific cell types also makes them attractive candidates for gene therapy.

There are many lipoplex preparations available currently, and a host of cationic lipids have been used in their formu-

lation (Lasic, 1997; Ruyschaert et al., 1994; Byk et al., 1998; MacDonald et al., 1999). Most formulations, in addition to the cationic lipid, incorporate at least one neutral or “helper” lipid, so-called because of their ability to improve transfectivity (Hui et al., 1996). Lipoplex microstructure has been shown to depend on the helper lipid. To date, two microstructure forms have been identified. One consists of lipid bilayers alternating with layers of DNA in a multilayer arrangement (Lasic et al., 1997; Radler et al., 1997, 1998; Boukhnikachvili et al., 1997; MacDonald et al., 1999). The other has an inverted hexagonal arrangement of cylinders with polar DNA cores each surrounded by a lipid monolayer (Koltover et al., 1998). Theoretical work has identified some of the factors contributing to the assembly of lipoplexes of the multilayer type (May and Ben-Shaul, 1997; Harries et al., 1998; May et al., 2000). The relationship between lipoplex microstructure and transfection efficiency has been examined (Lin et al., 2000).

As with most transfection systems, the rational design and use of lipoplexes is limited by our understanding of the process of complex formation, the structure, and stability of the complexes so formed and the manner in which they cross cell membranes and are relieved of their genetic freight. The objective of the current study was to address certain of these issues as applied to lipid-based vectors. The lipid chosen for examination was diC₁₄-amidine (Ruyschaert et al., 1994). It has been used successfully for in vitro transfection (Ruyschaert et al., 1994; El Ouahabi et al., 1996, 1997, 1999; Sasaki et al., 1997; Pector et al., 2000). Compared with many other cationic lipids, diC₁₄-amidine has the advantage that it does not require a helper lipid. This property significantly simplifies lipoplex formulation (Ruyschaert et al., 1994; El Ouahabi et al., 1997; MacDonald et al., 1999).

Submitted December 11, 2001, and accepted for publication February 20, 2002.

Address reprint requests to M. Caffrey, Biochemistry, Biophysics, and Chemistry, The Ohio State University, 100 West 18th Avenue, Columbus, OH 43210. Tel.: 614-292-8437; Fax: 614-298-1532; E-mail: caffrey.1@osu.edu.

© 2002 by the Biophysical Society

0006-3495/02/06/3105/13 \$2.00

Previous studies of the interaction of diC₁₄-amidine vesicles with plasmid DNA have shown it to involve at least two steps (Pector et al., 1998, 2000). The first is electrostatic and exothermic in nature and produces a soluble lipid/DNA complex. The second, slower step is endothermic and leads to what is referred to as a “fused complex.” The latter comes about as a result of charge neutralization of the contacting lipid and nucleic acid surfaces, which allows for the formation of a condensed complex. A flocculation process occurs at higher DNA/lipid ratios and at longer times after the lipoplex is formed.

Whereas insight into the assembly process was obtained in the latter study, the measurements performed were indirect and no detailed structure information emerged. This is what we set about providing in the current study. Specifically, we wished to determine the structure of the diC₁₄-amidine/DNA complex. For this purpose, static and time-resolved x-ray diffraction and polarized light microscopic measurements were performed. The microstructure of the complex was determined to be of a layered type with DNA duplexes sandwiched between lipid bilayers. The complex undergoes a thermotropic transition at 23°C, associated with a chain order/disorder rearrangement occurring within the bilayers.

In addition to a structure and thermotropic characterization, the diC₁₄-amidine/DNA complex used in this study was examined for its competency to transfect mammalian cells.

MATERIAL AND METHODS

DiC₁₄-amidine (molecular weight, 535 g/mol, Fig. 1) was synthesized as described (Ruysschaert et al., 1994). The lipid used in this study had a purity of 99% as established by ¹H-nuclear magnetic resonance and elemental analysis. The pcDNA3.1+, 5.4 kb, (Invitrogen, Carlsbad, CA), was amplified in *Escherichia coli*, and the circular plasmid was isolated and purified using a Qiafilter Plasmid Kit (Qiagen, Westburg, The Netherlands) according to the manufacturer's instructions. The concentration of plasmid DNA in 10 mM Hepes buffer (pH 7.3) was quantified by ultraviolet spectroscopy using the classical estimation $A_{260} = 1$ for 50 μg/mL for double-stranded DNA. The A_{260}/A_{280} ratio was always higher than 1.9, indicating that the sample was free of protein contamination and the final DNA concentration was close to 7 mg/mL. This corresponds to a nucleotide concentration of 22 mM, assuming an average molecular weight per nucleotide of 325 g/mol. For transfection experiments, the pCI vector (Promega, Genbank accession number U47120) with the luciferase gene inserted between the *EcoRI* and *NheI* sites of the multiple cloning site (resulting total length = 5.7 kb) was amplified and purified the same way as the pcDNA3.1 plasmid. All other chemicals were of analytical grade or better. For transfection experiments, the National Institutes of Health 3T3 cells were cultured in 24 well plates in Dulbecco's modified Eagle medium (#41965, Life Technologies/Gibco-BRL, Cleveland, OH) with 2 mM glutamine, 20 mM Hepes, 1% (v/v) penicillin/streptomycin (#15070, Life Technologies/Gibco-BRL) and 10% (v/v) bovine fetal serum (#10270, Life Technologies/Gibco-BRL). Transfection was performed in the same medium without serum and without antibiotics.

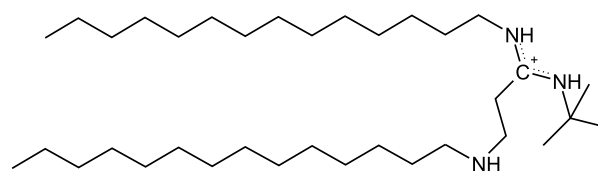


FIGURE 1 Molecular structure of diC₁₄-amidine.

Preparation of liposomes

Fifty milligrams of diC₁₄-amidine (dry powder, base form) were combined with 1 mL of 10 mM Hepes, unbuffered. The dispersion was heated to 65°C for 10 min, vortexed for 1 min, then stored on ice for 5 min, and adjusted to pH 7.3 at room temperature (22°C) using 3-μL portions of concentrated HCl. The heating/cooling cycle and pH adjustment were repeated four times and were necessary to produce a homogeneous, stable suspension at this concentration. Alternatively, a short sonication (Branson sonicator, microtip, four times 30 s, ~45°C, 1-min pause between cycles) was used in place of heating/cooling cycles, giving the same results.

X-ray samples

Lipid/DNA complexes were prepared by direct injection of the plasmid DNA (22 mM nucleotide, 7 mg/mL in Hepes buffer, pH 7.3) solution into a diC₁₄-amidine liposome (50 mg/mL in Hepes buffer) suspension contained in a 1-mm diameter quartz x-ray capillary (Charles Supper Co., Natick, MA or Mark-Rörchen, W.Müller, Berlin). Mixing was achieved using a 0.51 × 76.2-mm-long needle (model 25G3, Becton-Dickinson, Franklin Lakes, NJ). The capillaries were centrifuged for 2 min at ~2,000 × *g* (clinical centrifuge, IEC, Needham, MA) and room temperature to consolidate the sample. Capillaries were flame sealed using a microtorch (Microflame Inc, Minnetonka, MN). A small drop of extra fast epoxy glue (Hardman Inc., Belleville, NJ) was used to protect the fused tip and to ensure hermetic sealing. Capillaries were centrifuged again for 30 min at ~9,000 × *g* (Jouan MR14-11, Jouan Inc., Winchester, VA) at 20°C to sediment the CL-DNA complex for use in x-ray diffraction measurements. Samples were prepared with the following DNA/lipid ratios (ρ = DNA base/lipid (by mol)): 0 (pure lipid), 0.03, 0.21, 0.41, 0.6, 0.82, 1.65, and 3.3. Complexes prepared in this way will be referred as “intact complexes” to distinguish them from other preparations as described below.

To facilitate the x-ray diffraction measurements, it was established that a higher complex concentration than was produced using the above method was needed. To this end, a maximal volume of 73 μL of complex suspension prepared using the method described above was frozen at -80°C and lyophilized (16 h, 30 mTorr) while contained in an open capillary. The resulting dry powder (0.3–0.7 mg) was hydrated in 3 to 5 μL of 10 mM Hepes buffer (pH 7.3). The capillary was centrifuged for several minutes at ~2,000 × *g* and flame sealed as above. All operations after lyophilization were performed at room temperature (~20°C–25°C).

To prevent aggregation of individual complexes upon lyophilization another set of samples was prepared by lyophilization in the presence of sucrose. All manipulations were identical to those described above except that the complexes were formed in Hepes buffer containing 10% (w/v) sucrose.

Diffraction measurements

Most of the x-ray diffraction measurements were performed on a rotating anode generator (Rigaku RU-300, Rigaku U.S.A., Danvers, MA) operated at 45 kV and 250 mA and producing Ni-filtered (0.015-mm thick) Cu *K*_α radiation (wavelength λ = 1.5418 Å). The x-ray beam was focused by two

curved Ni-coated mirrors (Charles Supper Co., Natick, MA) to a spot size of $\sim 1.0 \times 0.5$ mm at the detector. Sample-to-detector distance was measured using a silver behenate standard (d_{001} , 58.4 Å; Blanton et al., 1995), and was usually set at 120 or 250 mm. High-resolution image plates (250×200 mm, HR-III_n, Fuji Medical Systems, U.S.A., Stamford, CT) were used to record diffraction patterns and were scanned using a phosphorimage scanner (Storm-840, Molecular Dynamics, Sunnyvale, CA) at a resolution of 100 μ m. At a sample-to-detector distance of 250 mm, it was possible to record simultaneously on the one plate both low- and wide-angle diffraction with a reciprocal vector space ranging from 4×10^{-2} Å⁻¹ to 1.84 Å⁻¹ (corresponding to real space ranging from 160–3.4 Å, respectively). Intensity versus scattering vector, $q = 4\pi \sin \theta / \lambda$, ($I - q$) plots were obtained by radial integration of static two-dimensional diffraction patterns using the FIT2D program (Hammersley et al., 1996). The Peakfit 4.0 program (SPSS Inc., Chicago, IL) was used to fit the $I - q$ plots and to find peak maxima and integrated intensities.

A home-built streak camera (Zhu and Caffrey, 1993) was used for time-resolved, temperature-scanning x-ray diffraction experiments. It consisted of a narrow vertical slit 2 to 3 mm wide and a stepper motor mechanism for continuously moving the image plate ~ 5 mm behind the slit at a translation rate of 0.5 mm/min.

Sample capillaries were placed in a home-built temperature-regulated holder designed to accommodate seven samples (Zhu and Caffrey, 1993). Sample temperature was regulated by two thermoelectric Peltier effect elements controlled by a computer feedback system. Temperature accuracy and stability were better than 0.1°C in the temperature range from 4°C to 60°C. Typical exposure times were 1 to 2 h.

Initial diffraction patterns were recorded after at least a 24-h equilibration period at 20°C. Subsequently, temperature was dropped to 4°C, and samples were incubated at this temperature for at least 2 h. Additional measurements were performed in the heating direction in steps of 5°C or 10°C. Samples were incubated at each new temperature for at least 2 h before an exposure. After completing the measurement at 60°C, sample temperature was returned to 20°C, and final exposures were taken after at least 2 h of incubation at this temperature.

Some of the diffraction measurements were performed on the ID-2 high brilliance beamline at the European Synchrotron Radiation Facility (ESRF, Grenoble, France) using 12.5-keV x-rays, whereas others used the X-12B beamline at the National Synchrotron Light Source (NSLS, Upton, NY) using 9-keV x-rays. At the ESRF, an image intensifier-CCD detector (1024×1024 pixels, 190-mm diameter, beam size at the sample position = 300×100 μ m, sample-to-detector distance = 150 cm) was used with a typical exposure time of 1 to 5 s. At NSLS, a gas wire two-dimensional detector (508×496 pixels, area = 10×10 cm (Capel et al., 1995), beam size at the sample position = 500×300 μ m, sample-to-detector distance = 70 cm) was used with an exposure time of 3 min.

Polarized light microscopy

Optical textures of lipid-DNA samples were examined using a polarizing light microscope (Model POS, Olympus America Inc., Melville, NY). Images were recorded with a color video camera (Panasonic GP-KR222, Matsushita Communication Industrial Co., Ltd., Yokohama, Japan) connected to a personal computer by means of a Meteor (Matrox Electronic Systems Ltd., Quebec, Canada) frame grabber. Pre-formed samples were transferred directly from x-ray capillaries to microscope slides and were covered with a glass coverslip. Extra buffer was added to the samples as necessary before placement of the coverslip to ensure full hydration for the duration of the experiment. Vacuum grease was placed between the slide and coverslip but not contacting the sample to provide hermetic sealing. The sample on the glass slide was placed into a microscope temperature-controlled holder (FP 84, Mettler Toledo, Columbus, OH). Temperature was measured by means of a thermocouple (BAT-12 with IT-23 probe, Physitemp Instruments, Inc., Clifton, NJ) placed in close proximity to the interrogated region of the sample.

Transfection assays

The National Institutes of Health 3T3 cells were cultured in 24 well plates at a density of 10^5 cells/well 24 h before transfection. The lipid/DNA complexes were prepared as follows: liposomes from the 50 mg/mL stock used for x-ray experiments were diluted to 40 μ g/mL in 10 mM Hepes containing 10% (w/v) sucrose. DNA was diluted to concentrations between 4.8 and 37 μ g/mL (according to the desired DNA/lipid ratio) in 10 mM Hepes and 10% (w/v) sucrose. Then, 250 μ L of lipid- and DNA-containing solutions were mixed together quickly with a pipettor and incubated at 20°C for 20 min to allow complex formation. The resulting complex suspension was frozen in liquid nitrogen and lyophilized (30 mTorr, 16 h). One-half hour before transfection, complexes were rehydrated with 0.5 mL of water and left on an orbital shaker at 150 rpm. Just before transfection, they were diluted twice with DMEM serum-free medium. The culture medium was carefully aspirated from the culture plate, and 200 μ L of the complex suspension were added to each well. After 2 h in the incubator at 37°C, the complexes were aspirated, and 1 mL complete medium was added. After 24 h, luciferase gene expression was quantified using the Luciferase Assay System of Promega according to the manufacturer's instructions. Luciferase activity was measured in a Turner Designs Lumimeter Model TD-20/20. Similar experiments were made with complexes lyophilized without sucrose and with nonlyophilized complexes.

RESULTS

Cationic lipid, diC₁₄-amidine

The phase properties and microstructure characteristics of the cationic lipid, diC₁₄-amidine, in isolation have not been examined in any detail previously. Such information is needed by way of understanding the nature of the complex it forms when combined with DNA. Our initial studies of the pure lipid were performed using rehydrated lyophilized samples as described under Materials and Methods. In the temperature range from 4°C to $\sim 40^\circ\text{C}$, the lipid existed in the lamellar crystal (L_c) or solid state. This is characterized by a series of equally spaced, sharp reflections in the corresponding low-angle diffraction pattern, and by several sharp wide-angle reflections (Fig. 2). The lamellar repeat spacing (d_{001}) for the L_c phase is 41.7 ± 0.1 Å. It is insensitive to temperature and hydration in the range studied.

Time-resolved x-ray diffraction measurements were made, which revealed an L_c -to-lamellar liquid crystal (L_α) phase transition occurring in the vicinity of 40°C (Fig. 3). The L_α phase had multiple, sharp low-angle diffraction peaks consistent with a one-dimensional lamellar periodicity. The wide-angle region of the pattern had a broad diffuse band centered at ~ 4.4 Å characteristic of "fluid" hydrocarbon chains. The streak image for the temperature scan indicated that the transition began at $\sim 39^\circ\text{C}$ and was complete at 43°C (Fig. 3). Static diffraction patterns recorded above the transition show that the lamellar repeat of the L_α phase ranges from 80 Å to greater than 250 Å (the upper limit detectable with the current experimental arrangement), depending on hydration level. Thus, the cationic lipid has the capacity to imbibe water and to swell while maintaining its lamellar structure upon chain melting. Cooling the sam-

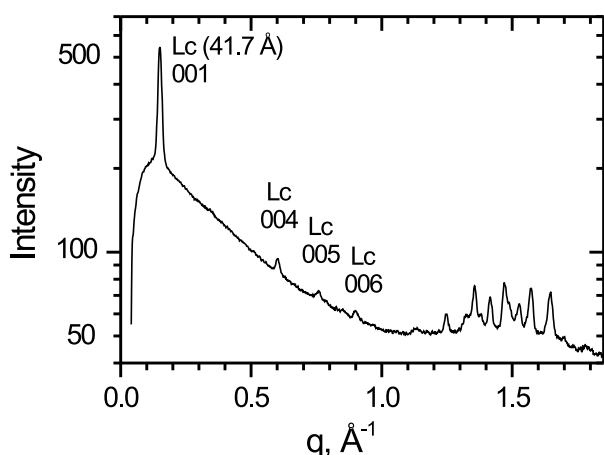


FIGURE 2 Low- and wide-angle x-ray diffraction from diC₁₄-amidine in excess 10 mM Hepes buffer, pH 7.3, at 20°C.

ple to 20°C triggered a transformation back to the *L_c* phase within minutes.

Mild sonication of a dispersion of diC₁₄-amidine in buffer above 40°C produced what are likely to be unilamellar vesicles. The vesicles remain stable for days and no detectable low-angle diffraction, indicative of multilayers, was seen with sonicated samples held for 3 days at 20°C when examined using a synchrotron x-ray source (Fig. 4 *A*). These are the same type of vesicles that were used in the preparation of DNA complexes for transfection and that condense into multilamellar structures when combined with DNA. A similar condensing effect was induced by raising the salt concentration (to 0.5 M NaCl) of a sonicated liposome dispersion of diC₁₄-amidine. This suggests that charge screening of the cationic amidine headgroup facilitates the collapse of isolated, like-charged membranes onto one another.

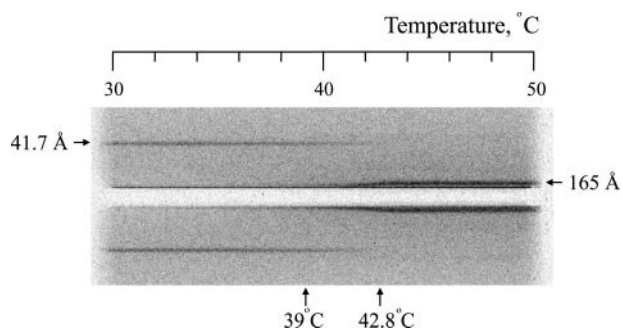


FIGURE 3 Time-resolved low-angle x-ray diffraction from diC₁₄-amidine in 10 mM Hepes buffer, pH 7.3, recorded as a function of temperature in the streak detector mode. The onset and completion temperatures of the *L_c*-to-*L_α* transition at 39°C and 42.8°C are indicated. The temperature scan rate was 6°C/h. The detector was translated behind a ~3-mm slit at a rate of 0.5 mm/min.

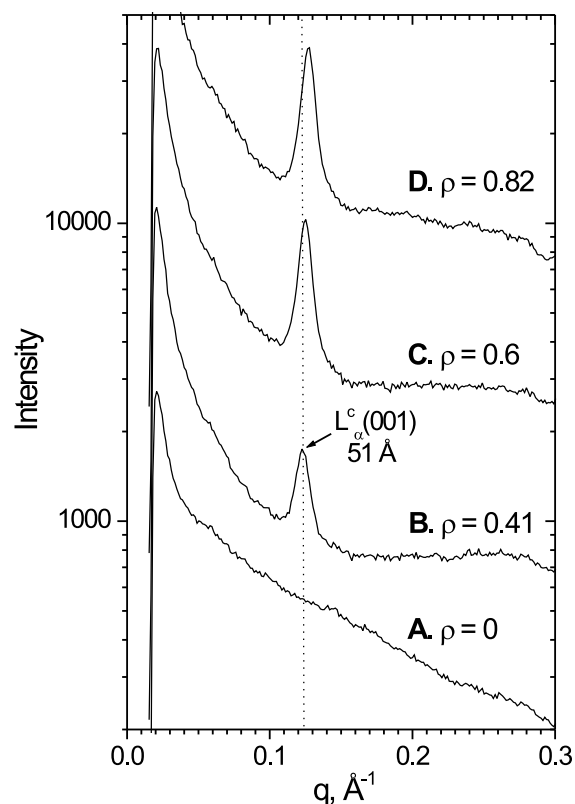


FIGURE 4 Diffraction curves from intact diC₁₄-amidine/DNA complexes in excess 10 mM Hepes buffer, pH 7.3, at the indicated DNA/lipid molar ratios, ρ , recorded using synchrotron radiation (NSLS) at 30°C.

diC₁₄-amidine/DNA complex

When liposomes of diC₁₄-amidine were combined with DNA, a complex was formed. The complex is characterized by a strong diffraction line centered at ~50 Å when monitored in a dilute suspension at 30°C (Fig. 4). The corresponding wide-angle region of the pattern is devoid of strong or sharp reflections suggesting, to within the sensitivity of the method, that the lipid acyl chains within the complex are “fluid.”

To visualize the complex, as well as other components in the system, the aforementioned dilute dispersion was concentrated by lyophilization followed by rehydration, as described under Materials and Methods. This procedure did not interfere with the original complex in the dilute suspension. However, the corresponding diffraction pattern (Fig. 5) now showed higher orders of what amounted to lamellar reflections from the complex and that are tentatively identified as being in the *L_α^c* phase (superscript *c* refers to complex following the notation in Koltover et al. (1998)). The lamellar repeat of the *L_α^c* phase remained at ~50 Å, as was observed before lyophilization.

In addition to the *L_α^c* phase, the concentrated complex also revealed the original *L_c* phase from uncomplexed lipid. The *L_c* phase gave rise to sharp reflections with a d_{001} of

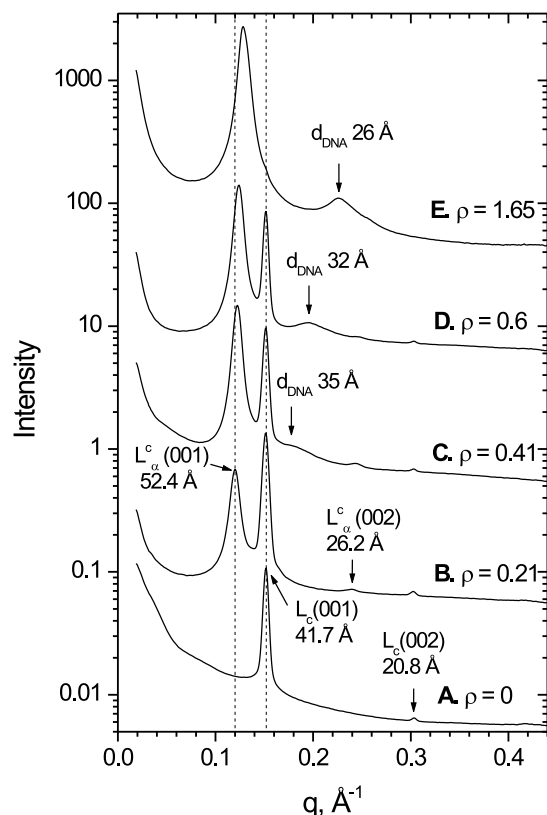


FIGURE 5 Diffraction curves from diC₁₄-amidine/DNA samples prepared by lyophilization in excess 10 mM Hepes buffer, pH 7.3, at the indicated DNA/lipid molar ratios, ρ , recorded using synchrotron radiation (ESRF) at 30°C.

41.7 Å, as before. As the DNA/lipid mole ratio, ρ , was increased, the amount of the L_c phase fell relative to that of the L_α phase from the complex, as expected (Fig. 6). Beyond $\rho = 0.8$, the L_c phase was no longer detectable, suggesting that the lipid had become completely saturated with DNA at this DNA/lipid ratio.

A third feature present in diffraction patterns of the lamellar lipid/DNA complexes was a relatively broad, low-angle band whose scattering angle was sensitive to ρ up to a value of 0.8 (Fig. 5). We ascribe this to a DNA-DNA spacing that is associated with the packing of DNA strands next to one another while sandwiched in the water layer between lipid bilayers. Such structures have been proposed to exist in DOPC-DOTAP/DNA complexes (Radler et al., 1997; Koltover et al., 1999). The broad band, hereafter identified as d_{DNA} , was barely recognizable at low ρ values where it was small and on the wide-angle shoulder of the first order peak of the lipidic L_c phase with a d_{DNA} value of 35 Å (Fig. 5 C). At higher values of ρ , it became stronger and more visible as it resolved itself from other lipid and complex reflections (Fig. 5 E). d_{DNA} reached a limiting value of 26 Å at high DNA loadings (Fig. 7 B). This value corresponds to the relatively close-packing of hydrated B-

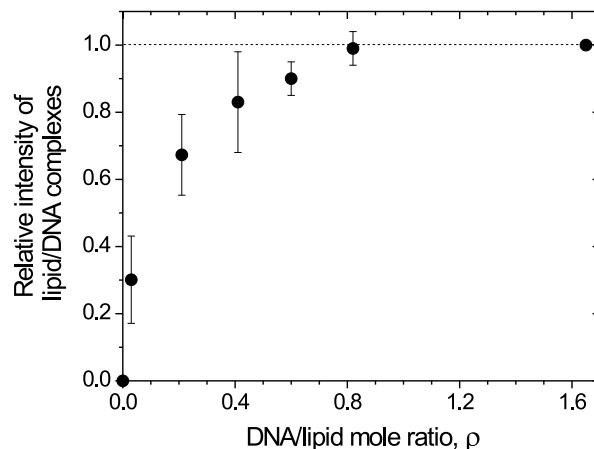


FIGURE 6 Dependence of the intensity of the first order small-angle reflection from diC₁₄-amidine/DNA complexes, $I_{L\alpha(001)}$, normalized to the sum of intensities of the first order reflection from the L_c phase, $I_{Lc(001)}$, and the first order reflection from the lipid/DNA complex, $I_{L\alpha(001)}$, $[I_{L\alpha(001)}/(I_{L\alpha(001)} + I_{Lc(001)})]$, on the DNA/lipid mole ratio, ρ .

DNA and is in agreement with previous results obtained with related systems (Radler et al., 1997; Koltover et al., 1999). The diameter of B-DNA is ~ 20 Å (Podgornik et al., 1989).

Interestingly, at $\rho = 1.65$ and 20°C, the diffraction pattern from the complex was dominated by two, relatively broad reflections. One was at 47 Å and the other was at 27 Å (Fig. 8, A and B). The spacing ratio of the two reflections is 1.74, approximately $\sqrt{3}$, reminiscent of a hexagonally packed structure. This is fortuitous, however, because the two reflections have disparate origins as is apparent from the titration studies represented in Fig. 5 and temperature variation in Fig. 8. The first of the two reflections is from the L_α phase of the complex, whereas the second derives from the one-dimensional DNA periodicity in the plane of its hosting L_α phase. The two reflections move to higher q values as ρ rises, but they do so at different rates. At the higher values of ρ , the latter masks the weaker second order reflection of the L_α phase.

Thermotropic behavior of diC₁₄-amidine/DNA complexes

The phase behavior of lipid/DNA complexes were examined by making simultaneous low- and wide-angle x-ray diffraction measurements in the temperature range from 4°C to 60°C. The wide-angle diffraction pattern was used to report on the state of order/disorder of hydrocarbon chains within the plane of lipid membranes. For lipid/DNA complexes at $\rho = 1.65$, the diffraction pattern had a single sharp reflection at 4.1 Å at temperatures from 4°C to $\sim 20^\circ\text{C}$ (Fig. 9). This is characteristic of the so-called gel phase where chains are rigid in the all-*trans* configuration. It is seen typically in the lamellar gel (L_β), ripple or undulated (P_β)

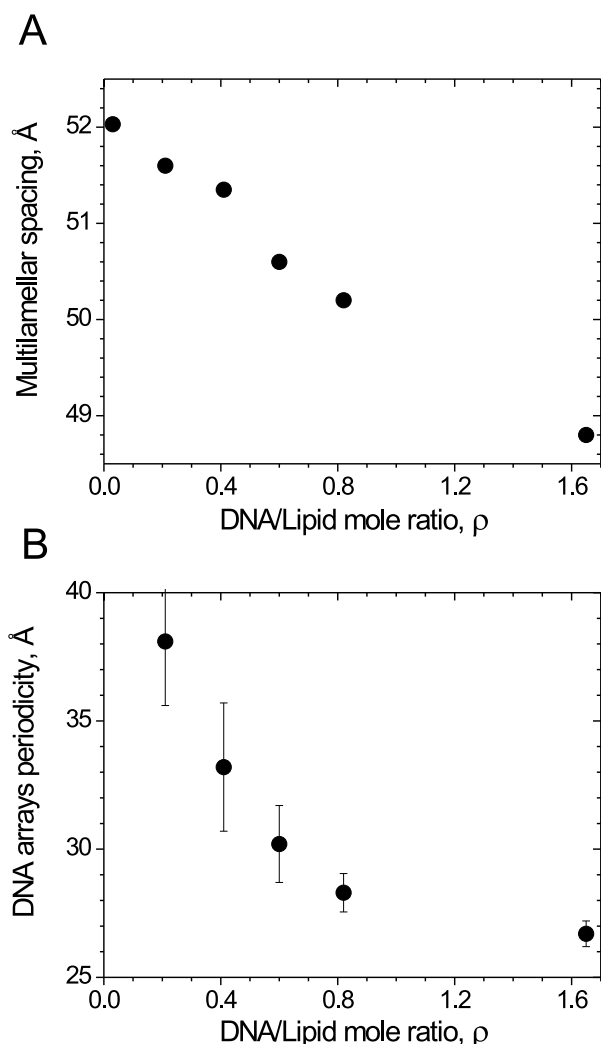


FIGURE 7 Dependence of multilamellar repeat distance at 30°C (A) and DNA-DNA spacing at 50°C (B) in diC₁₄-amidine/DNA complexes on temperature at a DNA/lipid mole ratio, ρ .

and the lamellar interdigitated ($L_{\beta i}$) phases (Tardieu et al., 1973). We refer to this low temperature modification as the L_{β}^c phase, following the notation introduced above.

Upon heating, the complex underwent a dramatic chain order/disorder transition to the L_{α}^c phase in the vicinity of 25°C (Fig. 9). The transition is associated with the loss of the sharp reflection at 4.1 Å and the appearance of a broad scattering peak centered at 4.4 Å, which is characteristic of fluid chains. The transition is captured quantitatively in Fig. 10, which shows an abrupt transformation in the wide-angle diffraction/scattering behavior at ~23°C. This coincides exactly with the transition temperature observed in a separate calorimetry measurement on essentially the same samples as used in the current study (Pector et al., 2000).

The change in the diffraction pattern at wide-angles was accompanied by another at low angles. The data in Fig. 8 A show that the lamellar repeat increased rapidly in the vicinity of the L_{β}^c -to- L_{α}^c transition between 20°C and 25°C. The

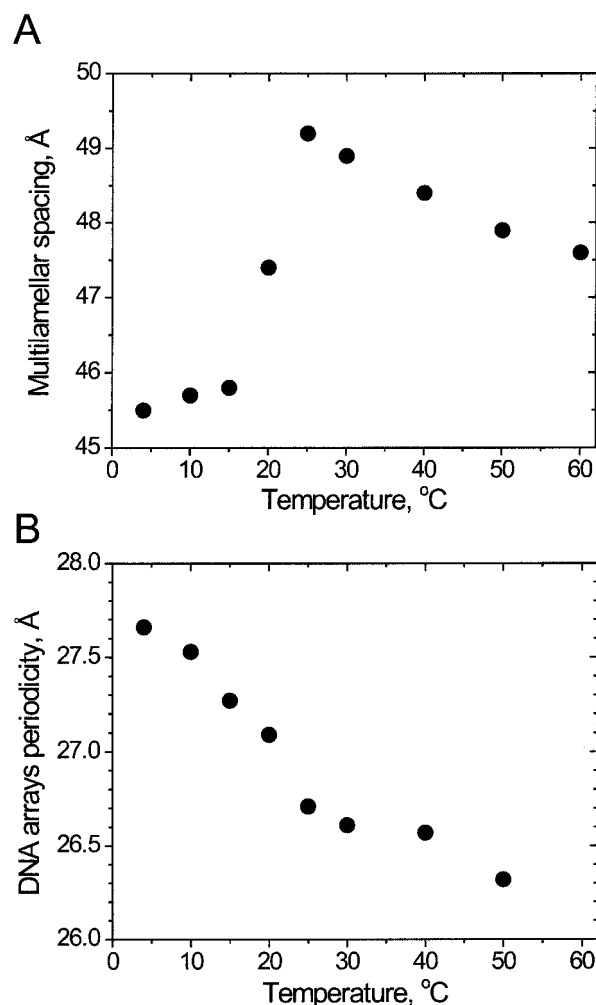


FIGURE 8 Dependence of multilamellar spacing (A) and DNA-DNA spacing (B) in diC₁₄-amidine/DNA complexes on temperature at a DNA/lipid mole ratio of 1.65.

ity of the L_{β}^c -to- L_{α}^c transition between 20°C and 25°C. The further fall of the lamellar repeat with increasing temperature above 25°C is typical of liquid crystal phases, of which the L_{α}^c phase is a member. It is usually attributable in part, at least, to the rising number of trans/gauche isomers along the length of the chains in the high temperature L_{α}^c phase.

The DNA-DNA strand spacing within the complex did change with temperature in the vicinity of the L_{β}^c -to- L_{α}^c transition (Fig. 8 B). However, the magnitude of change was small amounting to ~1 Å in the range from 4°C up to the transition at 25°C. Thereafter, d_{DNA} remained relatively constant at ~26.5 Å up to 50°C.

The L_c phase that is present in samples prepared with $\rho < 0.82$ underwent the chain order/disorder transition at 40°C. This is expected behavior for the free, unassociated lipid present in samples where there is a molar excess of lipid. What is interesting is that upon heating such samples through the 40°C transition, the original L_c phase was not

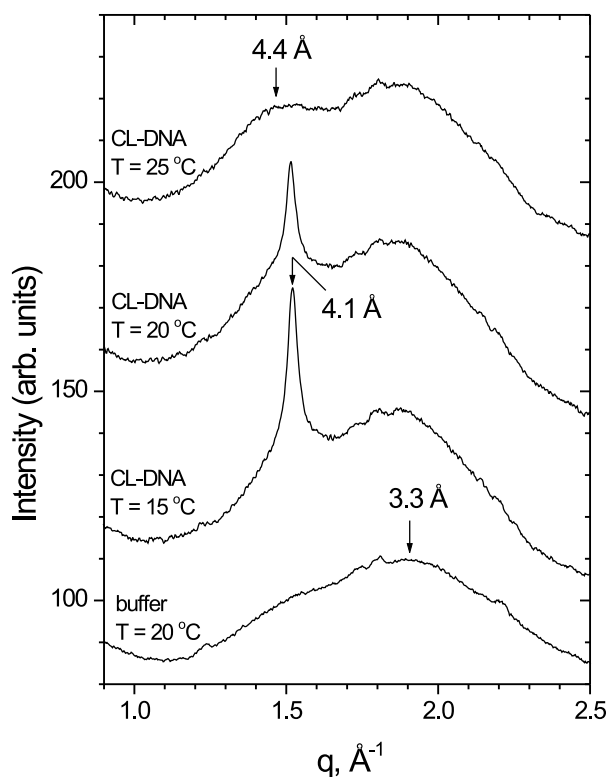


FIGURE 9 Wide-angle diffraction from diC₁₄-amidine/DNA complexes in buffer at a DNA/lipid mole ratio of 1.65 and from buffer alone recorded as a function of temperature in the vicinity of the lipid chain-melting transition.

recovered upon cooling and indeed upon incubation for at least one day at 20°C. This observation applies to all samples with $0.03 < \rho < 0.82$. Two possible explanations for this result come to mind. First, the free lipid transformed upon heating from the bulk L_c phase to dispersed thermally

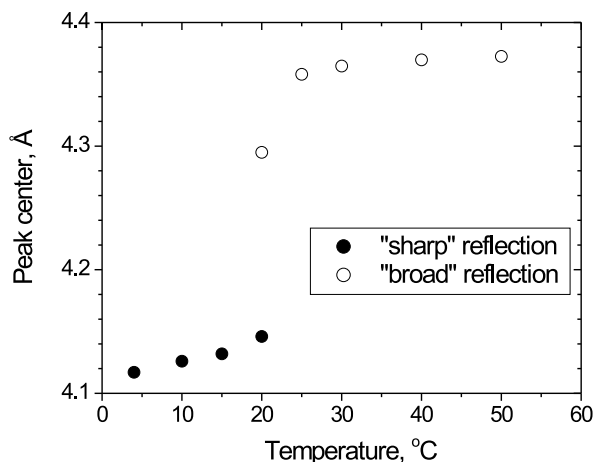


FIGURE 10 Change in the position of the wide-angle reflection as a function of temperature for diC₁₄-amidine/DNA complexes at a DNA/lipid mole ratio 1.65.

stable unilamellar vesicles that lack an ordered multilamellar structure and thus, the L_c diffraction signature. This seems unlikely since the transition undergone by the diC₁₄-amidine lipid in isolation at 40°C is reversible, as noted. The second possibility is that the fluidized lipid above the transition at 40°C “gains access” to the DNA and participates in complex formation. This new complex, with a lower ρ , remains intact upon cooling. Consistent with this hypothesis is the fact that the d_{DNA} increased upon cycling through 40°C, reflecting the drop in ρ for the complex. Thus, thermal history would appear to play a role in the assembly of the lipid/DNA complex, which, in turn, is likely to impact its properties as a vehicle for porting DNA into cells.

Effect of DNA concentration

As noted, the DNA carrying capacity of the diC₁₄-amidine lipid reached saturation at $\rho = 0.8$ when the lipid/DNA complex was formed following the standard preparation protocol. This result is based on a loss of diffraction, characteristic of the L_c phase from free lipid, observed when titrating the lipid with DNA (Fig. 6). Consistent with this is the reduction in the DNA spacing, which reached a limiting value of ~ 26 Å at $\rho = 0.8$ (Fig. 7 B). This is reasonable for the diameter of hydrated B-DNA and close to limiting values observed for DNA-DNA separations in separate but related studies (Radler et al., 1997). As might be expected, the reproducibility of the measured strand separation distance worsened as ρ decreased below 0.8 (Fig. 7 B). In a related study, free DNA was observed in the supernatant of centrifuged complexes prepared at $\rho > 0.6$ (Pector et al., 2000).

We also found that the lamellar repeat of the complex fell dramatically with increasing DNA content (Fig. 7 A). This amounts to a condensing effect where the positively charged membrane-associated lipid binds tightly to the polyanionic macromolecules. The net effect is to draw the lipid bilayers closer together with the likely expulsion of a certain amount of aqueous medium. What is surprising is that the effect continued beyond $\rho = 0.8$ where other characteristics of the system appeared to stabilize. In this case, the drop in the lamellar repeat continued out to, but not beyond, $\rho = 1.65$. A subsequent measurement made at $\rho = 3.3$, showed no change in d_{001} of the L_α phase compared with that at $\rho = 1.65$ (data not shown).

Domains size

A perusal of the data in Fig. 5 E shows that the diffraction peaks arising from both the one-dimensional lamellar and DNA periodicities in the lipid/DNA are quite broad. The width of a diffraction peak is related, among other things, to the size of the domains from which the diffraction comes (Zhang et al., 1994). The actual peak widths observed for

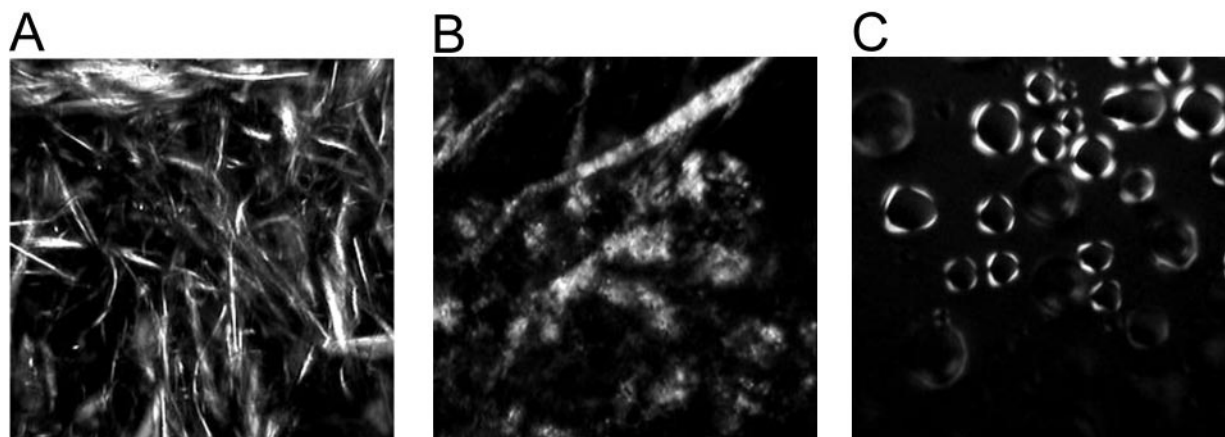


FIGURE 11 Polarized light microscopic images of diC₁₄-amidine and diC₁₄-amidine/DNA complexes in excess buffer. DiC₁₄-amidine alone at 25°C (A), diC₁₄-amidine/DNA complex at $\rho = 0.82$ and 25°C before heating (B), and after heating to 70°C and subsequent cooling to 25°C (C).

the lipid/DNA complex were three to four times the instrument (rotating anode x-ray source) resolution. They have been used to estimate the average domain size of the multilayers and the DNA arrays using the following relation:

$$L/d \approx q/\Delta q \quad (1)$$

in which L is the average domain size, d is the multilayer or DNA repeat distance, and Δq is the full-width-at-half-maximum of the diffraction peak in q space corrected for the resolution of the instrument. A more rigorous peak width analysis that includes peak fitting has been described (Roux and Safinya, 1988; Kaganer et al., 1991; Zhang et al., 1994). Using Eq. 1, we have determined that the average domain size of the multilayers and of the DNA arrays are 13.0 ± 1.5 lamellae and 8.5 ± 1 DNA strands, respectively. No significant dependence of average multilayer and DNA domain size on temperature or DNA concentration was found. The influence of sample preparation and thermal history on domain size was not investigated. The values reported above are comparable with those of other cationic lipid/DNA complexes (Radler et al., 1997; Schmutz et al., 1999).

Optical textures

Pure diC₁₄-amidine dispersed in HEPES buffer (pH 7.3) at room temperature appeared as strongly birefringent strands floating in a dark isotropic buffer when viewed with a microscope under crossed polarizers (Fig. 11 A). Heating the sample above 40°C caused the birefringent strands to disappear. The strands reappear upon cooling to 25°C. The lipid/DNA complexes with a high DNA content were also birefringent and exhibited the “oily streak” and “spherulite”-like defects characteristic of smectic or lamellar liquid crystals (Fig. 11 B) (Rosevear, 1954; Radler et al., 1998).

This corroborates the x-ray diffraction results presented above. Heating the complex above 70°C, and subsequent cooling to 25°C, produced air bubbles with uniaxial birefringence at their periphery (Fig. 11 C). The uniaxial texture is a fingerprint of the lamellar phase also (Rosevear, 1954).

Transfection studies

To compare the x-ray structure study with the known transfection properties of diC₁₄-amidine (Ruysschaert et al., 1994; El Ouahabi et al., 1996), complexes were made in the same way as for the diffraction experiments above except that a plasmid with the luciferase reporter gene, pCI-Luc, was used in place of the pcDNA3.1+. Complexes prepared in 10 mM HEPES, pH 7.3, were lyophilized and rehydrated with water and then mixed with culture medium without serum. The complexes after lyophilization and rehydration were devoid of transfection activity. This result is consistent with the observations of Li et al. (2000) and Allison and Anchordoquy (2000). They found that lyophilization significantly increased complex particle size, which suppressed transfection. However, lyophilization in the presence of 10% sucrose (other disaccharides had similar effects) was shown to prevent particle size growth and loss of transfection activity. To see if the same applied to our system, complexes were prepared following the standard protocol but in the presence of 10% sucrose. The samples were subsequently lyophilized and rehydrated in water. A comparison of the transfection activity of the intact complexes (prepared without lyophilization) and those prepared by lyophilization in the presence of sucrose is shown in Fig. 12. Both sample types behaved in the same way. The absolute transfection activities are the same as is the dependence of activity on DNA/lipid ratio, which is maximum at $\rho = 0.4$.

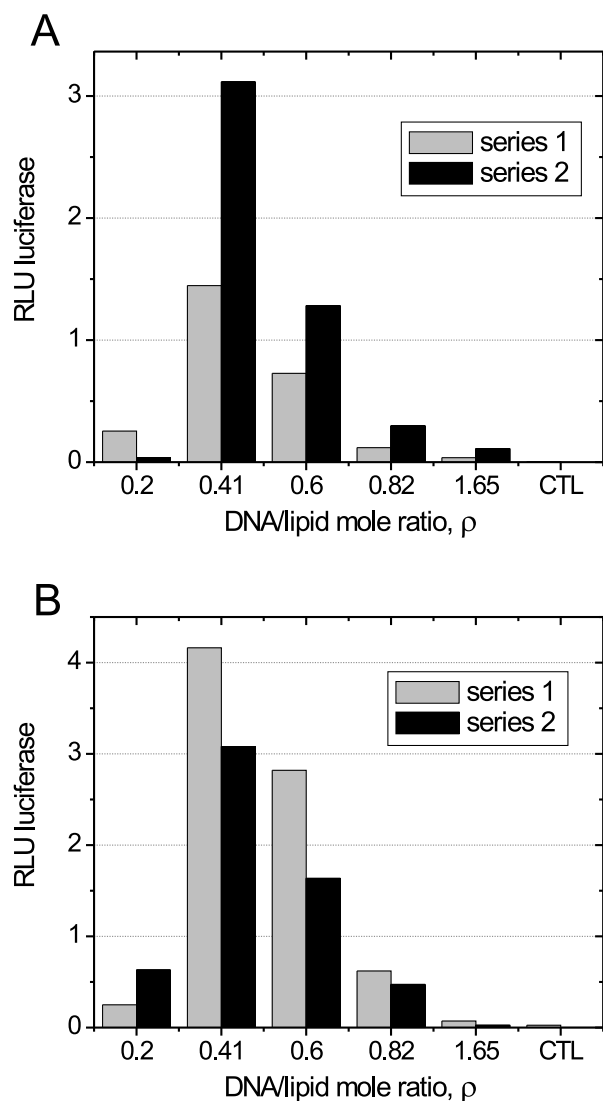


FIGURE 12 Transfection of National Institutes of Health 3T3 cells with diC14-amidine/DNA complexes as a function of the DNA/lipid mole ratio. Activity is measured as the luminescence of the expressed luciferase. RLU, Relative luminescence units. The experiment was performed in duplicate (series 1 and 2). (A) Intact complexes. (B) Complexes lyophilized in the presence of sucrose and rehydrated.

Structure of lipid/DNA complexes lyophilized with sucrose

Because the complexes lyophilized in the presence and absence of sucrose behaved differently in transfection we set out to determine if sucrose modified the microstructure of the complex. Accordingly, complexes were lyophilized in the presence of sucrose at different DNA/lipid ratios and diffraction patterns were recorded at 15°C, 30°C, and 50°C. All of the patterns and corresponding microstructure parameters were identical to those obtained for samples lyophilized in the absence of sucrose. These measurements confirm that the only effect of lyophilization in the absence of

sucrose was presumably to cause aggregation. However, aggregation had no effect on phase identity or microstructure.

DISCUSSION

Structure and thermal analysis

X-ray diffraction and polarized light microscopy were used to investigate the phase properties and microstructure of complexes formed between the cationic lipid, diC₁₄-amidine, and DNA. The results are consistent with a multilamellar arrangement of lipid bilayers where DNA strands are intercalated between them forming a separate, one-dimensional periodic array. Similar structures have been reported for complexes of DNA with cationic lipid (MacDonald et al., 1999) and in combination with neutral, so-called helper lipid (Radler et al., 1997).

In the current study, it proved difficult to investigate lipid/DNA complex formation using x-ray diffraction with samples prepared directly from sonicated lipid dispersions. In this case, the samples were too dilute and the uncomplexed or free lipid remained as unilamellar vesicles with no measurable diffraction signal. To overcome these problems, the lipid/DNA-containing samples were concentrated by lyophilization post-complex formation. A limited rehydration produced a significantly more concentrated sample from which readily measurable and interpretable diffraction could be obtained. This treatment, in addition to concentrating the sample, caused the uncomplexed and presumably vesicularized lipid to form a bulk lamellar phase, which at low temperature (below 40°C) was of the solid or L_c type. This alternate form of the free lipid could now be readily “seen” and monitored by x-ray diffraction.

Whereas the lyophilization/rehydration treatment affected the uncomplexed lipid as above, no noticeable change in the structure of the lipid/DNA complex was observed. Indeed, the first order, low-angle diffraction peak from the L_c phase of the complex remained essentially unchanged by the process (Figs. 4 and 5). Further, the response of this prominent diffraction feature to changes in DNA loading and to temperature was the same before and after the treatment.

The multilamellar lipid/DNA complex underwent a transition in the temperature range between 20°C and 25°C. This was ascribed to a “fluidization” of the lipid chains and was evidenced by a change in wide-angle diffraction from a single sharp reflection at 4.1 Å to a broad diffuse band centered at 4.4 Å (Fig. 9). The low-angle diffraction pattern changed through the transition also. In this case, it began with a d_{001} of ~46 Å below 20°C, rose to a maximum of ~50 Å at 25°C, and then decreased slowly with increasing temperature above 30°C (Fig. 8 A). The low temperature phase was identified as being of the L_β type with fully extended chains in the all-*trans* configuration. Above 25°C, the complex was identified as being in the L_α phase.

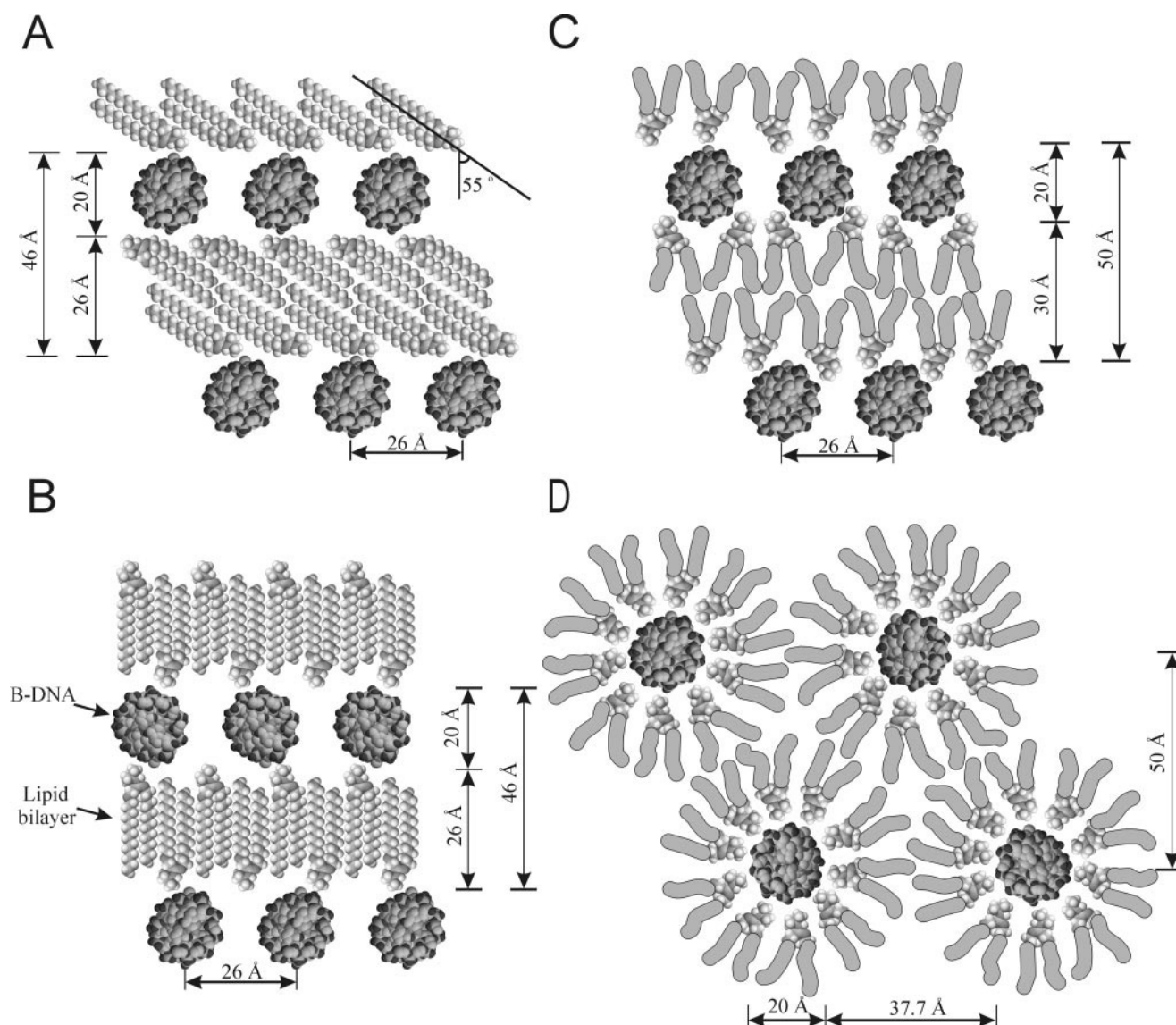


FIGURE 13 Molecular models of the diC₁₄-amidine lipid/DNA complex. Two possible arrangements below the lipid chain melting transition temperature, 23°C, are shown in *A* and *B*. They both represent multilamellar structures, with either tilted (*A*) or interdigitated chains (*B*), where DNA is intercalated between lipid bilayers. The high temperature arrangement is shown in *C* where the lipid chains are in the disordered state but the overall organization is multilamellar. Shown in *D* is an inverted hexagonal phase with DNA strands inside the water channels. This structure is included for comparative purposes only. Neither the x-ray diffraction nor the polarized microscopy studies provided support for the hexagonal arrangement.

Molecular model

By way of deciphering the detailed structure of the complex, it is necessary to work within the confines of established dimensions for the units that go to make up such complexes. With reference to Fig. 13, we see that the projected length per methylene ($-\text{CH}_2-$) group in a fully extended hydrocarbon chain is 1.27 Å. The lipid headgroup has an estimated maximal dimension of 4 to 5 Å. Thus, an arrangement in which the long-axis of the lipid is normal to the lamellar plane and the lipids are not interdigitated would produce a bilayer with a maximal thickness of 44 Å. This calculation

is for the pure, nonhydrated lipid and matches the corresponding experimental value of 42 Å (lipid chains in the L_c phase are possibly slightly tilted) recorded for the L_c phase of pure diC₁₄-amidine (Fig. 5 *A*). However, a value of ~46 Å was observed for the lipid/DNA complex at 20°C (Fig. 8 *A*). This dimension is not at all consistent with a multilamellar structure having untilted and noninterdigitated chains within the bilayer given that double-stranded DNA of the B type, as is assumed to exist in the complex, has a diameter of ~20 Å (Podgornik et al., 1989). The minimal dimension for such a complex is ~64 Å, assuming that the DNA and lipid are in direct contact and devoid of bridging water.

In light of this latter result, an alternate arrangement of lipid molecules within the complex must be considered. A complex of DNA sandwiched between lipid lamellae with a multilamellar repeat distance of ~ 46 Å and where the DNA strand has a diameter of 20 Å could possibly arise if the hydrocarbon chains were tilted and/or the lipid molecules were interdigitated across the bilayer midplane. Lipidic mesophases with tilted and interdigitated chains are common (Slater and Huang, 1991). It seems reasonable therefore to suggest the existence of such a structure for the current diC₁₄-amidine/DNA complex. A model incorporating a tilted lipid configuration would require an angle of $\sim 55^\circ$ between the bilayer normal and the long axis of the lipid molecule (Fig. 13 *A*). Interdigitation to the extent of almost full long-axis length of the lipid molecule must occur if it alone were to account for the structure of the complex (Fig. 13 *B*).

These calculations are based on a model in which the lipid bilayer surface and the surface of the DNA strand are in direct contact. Enhanced lipid tilting or interdigitation or a combination of the two would allow for hydration layers to be accommodated between the lipid and the DNA binding surfaces.

The above model that incorporates tilting and/or interdigitation is consistent with the measured lamellar repeat of ~ 46 Å in the L_β^c phase. Upon chain melting, the lamellar repeat increases by 4 Å and then decreases slowly with heating above the transition (Fig. 8 *A*). These structural changes can be accounted for by a relaxation of tilting and/or interdigitation upon fluidization of the hydrocarbon chains at the transition (Fig. 13 *C*). A rising level of *trans*/*gauche* isomerization along the length of the chain, which accompanies heating in the L_α phase, is consistent with the slow drop in *d*-spacing above the transition.

The model presented above for the intercalation of DNA strands between cationic lipid bilayers postulates directly contacting surfaces without intervening hydration layers. However, within the plane of the lamellae and between the strands of DNA is likely to reside an aqueous medium whose extent depends on the loading of the complex with DNA. This feature of the complex shows up as a decreasing strand separation with increasing DNA/lipid ratio (ρ), which reached a limiting value of ~ 26 Å at $\rho = 0.8$ (Fig. 7 *B*). If the DNA in the complex is of the B type with a diameter of ~ 20 Å (Podgornik et al., 1989), then the space between adjacent strands under maximal DNA loading conditions would be enough (~ 6 Å) to accommodate two to three water molecule shells (Fig. 13).

Comparison with other studies

The L_β^c -to- L_α^c transition observed for the lipid/DNA complex at $\sim 23^\circ\text{C}$ in this study (Fig. 10) corroborates quantitative results obtained using differential scanning calorimetry on similar complexes (Pector et al., 2000). In the latter

work, the calorimetrically determined transition temperature at $\sim 23^\circ\text{C}$ proved relatively insensitive to the DNA/lipid ratio although the enthalpy change of the transition fell precipitously with DNA loading. It essentially disappeared at $\rho = 1$. The authors interpreted these and other results as supporting a model in which lipid vesicles are destroyed in the process of forming the complex that has DNA strands surrounded by cationic lipid bilayers.

In contrast, the results presented in the current study strongly favor a complex that has a multilayered structure. This is based on both low-angle x-ray diffraction measurements (Fig. 5) and on polarized light microscopic examination of fully elaborated complexes (Fig. 11). The diffraction data show two reflections that index as the (001) and (002) reflections of a structure with lamellar periodicity. It is possible that these could derive from the (10) and (20) reflections of a hexagonal phase in which the (11) reflection was weak and thus masked by scattering from other structures in the sample. To facilitate the discussion, a molecular model for a hexagonal complex is presented in Fig. 13 *D*. It fits reasonably well with the dimensions found by the x-ray diffraction. However, in the case of the hexagonal structure, DNA-DNA strand separation reflections will not be present in contrast to what is clearly seen on the x-ray diffraction patterns in Fig. 5, *C* to *E*. Also the polarized light microscopic measurements show birefringence from the complex that is characteristically lamellar or smectic at 25°C , both before and after heating through the L_β^c -to- L_α^c transition (Fig. 11). We conclude therefore that the diC₁₄-amidine/DNA complex has a lamellar microstructure of the type shown in Fig. 13, *A* or *B*, below the phase transition and of the type shown in Fig. 13 *C* above the transition temperature.

Critical DNA/lipid ratio and its possible biological relevance

The results presented in this report identify a DNA/lipid mole ratio (ρ) of 0.8 as the end point for complex formation. At higher ratios, most measured parameters of the complex were found to stabilize and were no longer sensitive to ρ . Until now, all of our transfection experiments carried out *in vitro* have shown a maximal activity for $\rho = 0.4$ to 0.8 (Pector et al., 2000; Fig. 12). Complexes with $\rho = 0.4$ to 0.8 have a net positive charge (charge neutralization at $\rho = 1$). It was suggested (Bally et al., 1999) that positive charge facilitates complex binding to cell membranes and thus favors transfection. Charge repulsion should minimize complex aggregation, which will also contribute to enhanced transfectivity (Li et al., 2000; Allison and Anchordoquy, 2000). For $\rho < 0.8$, we see free lipid forming the L_c phase and so the exact DNA/lipid ratio in the complex is not known. However, because DNA-DNA separation increases with decreasing ρ below 0.8, we conclude that the DNA/lipid ratio in the complex also decreases and the complex becomes more cationic. A further reduction in the DNA load gives rise to a lower com-

plex yield and to complexes with lower DNA density. Thus, in our system a DNA/lipid molar ratio of 0.4 to 0.8 represents a compromise between competing effects where transfection efficiency is maximized.

Effect of lyophilization on transfection activity and complex structure

We found that lyophilized and rehydrated lipid/DNA complexes lost transfection activity. The effect was attributed to the aggregation of complexes upon lyophilization (Li et al., 2000; Allison and Anchordoquy, 2000). However, complexes lyophilized in the presence of sucrose-retained transfectivity suggesting that sucrose prevents complex aggregation. X-ray diffraction measurements showed that lyophilization, performed with or without sucrose, had no effect on complex phase state or phase microstructure.

CONCLUSIONS

The cationic lipid, diC₁₄-amidine, is used as a vehicle for porting DNA into cells for purposes of transfection. The complex formed between negatively charged DNA and the positively charged lipid has been characterized structurally by means of low- and wide-angle x-ray diffraction and by polarized light microscopy. The data suggest that the complex exists as a multilamellar array of lipid bilayers stacked one atop the other, each separated by a polar layer containing B-type DNA double helices and aqueous medium. The current model of the complex has lipid forming a tight complex with the DNA where the two make contact. Within the complex, the lipid chains are tilted with respect to the lamellar plane normal and/or are interdigitated across the bilayer midplane. The lipid component of the complex underwent a thermotropic transition at 23°C, which corresponds to a chain order/disorder transformation within the bilayer. The transition temperature was independent of DNA loading. Within the polar nucleic acid-containing layer, DNA polymers run parallel to one another. They are equally spaced giving rise to a one-dimensional array of cylindrical strands whose direction of periodicity is normal to that of the hosting lipid multilayer. The separation between DNA strands is sensitive to the nucleic acid loading of the complex and reaches a minimal value of 26 Å at a DNA (nucleotide)/lipid molar ratio of 0.8.

It was found that complexes lose significant transfection activity after lyophilization and rehydration. Addition of 10% sucrose before lyophilization prevents this deactivation. X-ray diffraction confirmed that the microstructure of the complexes does not change upon lyophilization with or without sucrose. We conclude that the main effect of sucrose is to prevent complexes from aggregating during lyophilization and preserves suitably sized complex particles for transfection.

Maximal transfection activity for intact complexes and for complexes lyophilized in the presence of sucrose was found to occur at a DNA/lipid ratio of 0.4. Under these conditions, complexes bear a net positive charge, which stabilizes them in dispersion, facilitates binding to target cell membranes, and supports maximal transfection efficiency.

We thank the members of our group J. Clogston and Y. Misquitta for invaluable input on this work. We are grateful to M. Capel (NSLS, Upton, NY) and N. Theyencheri (ESRF, Grenoble, France) for technical assistance. This work was funded in part by the National Institutes of Health (GM56969, GM61070), the National Science Foundation (DIR9016683, DBI9981990), and the Belgian FRiA and FNRS. M. Vandenbranden is a FNRS Research Associate.

REFERENCES

- Allison, S. D., and T. J. Anchordoquy. 2000. Mechanisms of protection of cationic lipid-DNA complexes during lyophilization. *J. Pharm. Sci.* 89:682–691.
- Bally, M. B., P. Harvie, F. M. P. Wong, S. Kong, E. K. Wasan, and D. L. Reimer. 1999. Biological barriers to cellular delivery of lipid-based DNA carriers. *Adv. Drug Deliv. Rev.* 38:291–315.
- Blanton, T. N., T. C. Huang, H. Toraya, C. R. Hubbard, S. B. Robie, D. Louer, H. E. Gobel, G. Will, R. Gilles, and T. Raftery. 1995. JCPDS-international centre for diffraction data robin study of silver behenate: a possible low-angle x-ray diffraction calibration standard. *Powder Diffraction*. 10:91–100.
- Bleziinger, P., B. Freimark, M. Matar, E. Wilson, A. Singhal, W. Min, L. Nordstorm, and F. Pericle. 1999. Intratracheal administration of interleukin 12 plasmid-cationic lipid complexes inhibits murine lung metastases. *Hum. Gene Ther.* 10:723–731.
- Boukhnikachvili, T., O. Aguerre-Chariol, M. Airiau, S. Lesieur, M. Ollivon, and J. Vacus. 1997. Structure of in-serum transfecting DNA-cationic lipid complexes. *FEBS Lett.* 409:188–194.
- Byk, G., C. Dubertret, V. Escriou, M. Frederic, G. Jaslin, R. Rangara, B. Pitard, J. Crouzet, P. Wils, B. Schwartz, and D. Schermann. 1998. Synthesis, activity, and structure-activity relationship studies of novel cationic lipids for DNA transfer. *J. Med. Chem.* 41:224–235.
- Capel, M. S., G. C. Smith, and B. Yu. 1995. One- and two-dimensional x-ray detector systems at NSLS beam line X12B, for time-resolved and static x-ray diffraction studies. *Rev. Sci. Instrum.* 66:2295–2299.
- El Ouahabi, A., V. Pector, R. Fuks, M. Vandenbranden, and J. M. Ruyschaert. 1996. Double long-chain amidine liposome-mediated self replicating RNA transfection. *FEBS Lett.* 380:108–112.
- El Ouahabi, A., M. Thirty, V. Pector, R. Fuks, J. M. Ruyschaert, and M. Vandenbranden. 1997. The role of endosome destabilizing activity in the gene transfer process mediated by cationic lipids. *FEBS Lett.* 414:187–192.
- El Ouahabi, A., M. Thiry, S. Schiffmann, R. Fuks, H. Nguyen-Tran, J. M. Ruyschaert, and M. Vandenbranden. 1999. Intracellular visualization of BrdU-labeled plasmid DNA/cationic liposome complexes. *J. Histochem. Cytochem.* 47:1159–1166.
- Felgner, J. H., R. Kumar, C. N. Sridhar, C. J. Wheeler, Y. J. Tsai, R. Border, P. Ramsey, M. Martin, and P. L. Felgner. 1994. Enhanced gene delivery and mechanism studies with a novel series of cationic lipid formulations. *J. Biol. Chem.* 269:2550–2561.
- Felgner, P. L. 1997. Nonviral strategies for gene therapy. *Sci. Am.* 276:102–106.
- Gao, X., and L. Huang. 1995. Cationic liposome-mediated gene transfer. *Gene Ther.* 2:710–722.
- Hammersley, A. P., S. O. Svensson, M. Hanfland, A. N. Fitch, and D. Hausermann. 1996. Two-dimensional detector software: from real detector to idealized image or two-theata scan. *High Pressure Res.* 14:235.

- Harries, D., S. May, W. M. Gelbart, and A. Ben-Shaul. 1998. Structure, stability, and thermodynamics of lamellar DNA-lipid complexes. *Biophys. J.* 75:159–172.
- Hoffman, D. M. J., and R. A. Figlin. 2000. Intratumoral interleukin 2 for renal-cell carcinoma by direct gene transfer of a plasmid DNA/DMRIE/DOPE lipid complex. *World J. Urol.* 18:152–156.
- Hui, S. W., M. Langner, Y. L. Zhao, P. Ross, E. Hurley, and K. Chan. 1996. The role of helper lipids in cationic liposome-mediated gene transfer. *Biophys. J.* 71:590–599.
- Kaganer, V. M., B. I. Ostrovskii, and W. H. De Jeu. 1991. X-ray scattering in smectic liquid crystals: from ideal to real structure effects. *Phys. Rev. A.* 44:8158–8166.
- Koltover, I., T. Salditt, J. O. Radler, and C. R. Safinya. 1998. An inverted hexagonal phase of cationic liposome-DNA complexes related to DNA release and delivery. *Science.* 281:78–81.
- Koltover, I., T. Salditt, and C. R. Safinya. 1999. Phase diagram, stability, and overcharging of lamellar cationic lipid-DNA self-assembled complexes. *Biophys. J.* 77:915–924.
- Lasic, D. D. 1997. Recent developments in medical applications of liposomes: sterically stabilized liposomes in cancer therapy and gene delivery in vivo. *J. Contr. Release.* 48:203–222.
- Lasic, D. D., H. H. Strey, M. C. A. Stuart, R. Podgornik, and P. M. Frederik. 1997. The structure of DNA-liposome complexes. *J. Am. Chem. Soc.* 119:832–833.
- Li, B., S. Li, Y. Tan, D. B. Stolz, S. C. Watkins, L. H. Block, and L. Huang. 2000. Lyophilization of cationic lipid-protamine-DNA (LPD) complexes. *J. Pharm. Sci.* 89:355–364.
- Lin, A. J., N. L. Slack, A. Ahmad, I. Koltover, C. X. George, C. E. Samuel, and C. R. Safinya. 2000. Structure and structure-function studies of lipid/plasmid DNA complexes. *J. Drug Target.* 8:13–27.
- Liu, F., H. Qi, L. Huang, and D. Liu. 1997. Factors controlling the efficiency of cationic lipid-mediated transfection in vivo via intravenous administration. *Gene Ther.* 4:517–523.
- Logan, J. J., Z. Bebok, L. C. Walker, S. Peng, P. L. Felgner, C. J. Wheeler, G. P. Siegal, R. A. Frizzell, J. Dong, M. Howard, S. Matalon, M. Duvall, and E. J. Sorscher. 1995. Cationic lipids for reporter gene and CFTR transfer to rat pulmonary epithelium. *Gene Ther.* 2:38–49.
- MacDonald, R. C., G. W. Ashley, M. M. Shida, V. A. Rakhmanova, Y. S. Tarahovsky, D. P. Pantazatos, M. T. Kennedy, E. V. Pozharski, K. A. Baker, R. D. Jones, H. S. Rosenzweig, K. L. Choi, R. Qiu, and T. J. McIntosh. 1999. Physical and biological properties of cationic triesters of phosphatidylcholine. *Biophys. J.* 77:2612–2629.
- May, S., and A. Ben-Shaul. 1997. DNA-lipid complexes: stability of honeycomb-like and spaghetti-like structures. *Biophys. J.* 73:2427–2440.
- May, S., D. Harries, and A. Ben-Shaul. 2000. The phase behavior of cationic lipid-DNA complexes. *Biophys. J.* 78:1681–1697.
- Pector, V., J. Backmann, D. Maes, M. Vandenbranden, and J. M. Ruyschaert. 2000. Biophysical and structural properties of DNA-diC14-amidine complexes: influence of the DNA/lipid ratio. *J. Biol. Chem.* 275:29533–29538.
- Pector, V., J. Caspers, S. Banerjee, L. Deriemaeker, R. Fuls, A. El Ouahabi, M. Vandenbranden, R. Finsy, and J. M. Ruyschaert. 1998. Physico-chemical characterization of a double long-chain cationic amphiphile (Vectamidine) by microelectrophoresis. *Biochim. Biophys. Acta.* 1372:339–346.
- Podgornik, R., D. C. Rau, and V. A. Parsegian. 1989. The action of interhelical forces on the organization of DNA double helices: fluctuation-enhanced decay of electrostatic double-layer and hydration forces. *Macromolecules.* 22:1780–1786.
- Radler, J. O., I. Koltover, A. Jamieson, T. Salditt, and C. R. Safinya. 1998. Structure and interfacial aspects of self-assembled cationic lipid-DNA gene carrier complexes. *Langmuir.* 14:4272–4283.
- Radler, J. O., I. Koltover, T. Salditt, and C. R. Safinya. 1997. Structure of DNA-cationic liposome complexes: DNA intercalation in multilamellar membranes in distinct interhelical packing regimes. *Science.* 275:810–814.
- Rosevear, F. B. 1954. The microscopy of the liquid crystalline neat and middle phases of soaps and synthetic detergents. *J. Am. Oil Chem. Soc.* 31:628–639.
- Roux, D., and C. R. Safinya. 1988. A synchrotron x-ray study of competing undulation and electrostatic interlayer interactions in fluid multilamellar lyotropic phases. *J. Phys. France.* 49:307–318.
- Ruyschaert, J. M., A. El Ouahabi, V. Willeaume, G. Huez, R. Fuks, M. Vandenbranden, and P. Di Stefano. 1994. A novel cationic amphiphile for transfection of mammalian cells. *Biochem. Biophys. Res. Commun.* 203:1622–1628.
- Sasaki, S., J. Fukushima, H. Arai, K. Kusakabe, K. Hamajima, N. Ishii, F. Hirahara, K. Okuda, S. Kawamoto, J. M. Ruyschaert, M. Vandenbranden, B. Wahren, and K. Okuda. 1997. Human immunodeficiency virus type-1-specific immune responses induced by DNA vaccination are greatly enhanced by mannan-coated diC14-amidine. *Eur. J. Immunol.* 27:3121–3129.
- Schmutz, M., D. Durand, A. Debin, Y. Palvadeau, A. Etienne, and A. R. Thierry. 1999. DNA packing in stable lipid complexes designed for gene transfer imitates DNA compaction in bacteriophage. *Proc. Natl. Acad. Sci. U. S. A.* 96:12293–12298.
- Slater, J. L., and C-h. Huang. 1991. Lipid bilayer interdigitation. In *The Structure of Biological Membranes*. P. Yeagle, editor. CRC Press, Boca Raton, FL. 175–210.
- Tardieu, A., V. Luzzati, and F. C. Reman. 1973. Structure and polymorphism of the hydrocarbon chains of lipids: lecithin-water phases. *J. Mol. Biol.* 75:711–733.
- Zelphati, O., L. S. Uyechi, L. G. Barron, and F. C. J. Szoka. 1998. Effect of serum components on the physico-chemical properties of cationic lipid/oligonucleotide complexes and on their interactions with cells. *Biochim. Biophys. Acta.* 1390:119–133.
- Zhang, R., R. M. Suter, and J. F. Nagle. 1994. Theory of the structure factor of lipid bilayers. *Phys. Rev. E.* 50:5047–5060.
- Zhu, T., and M. Caffrey. 1993. Thermodynamic, thermomechanical, and structural properties of a hydrated asymmetric phosphatidylcholine. *Biophys. J.* 65:939–954.